EVALUATION MODEL FOR RESTRAINT EFFECT OF PRESSURE INDUCED BENDING ON THE PLASTIC CRACK OPENING OF A CIRCUMFERENTIAL THROUGH-WALL CRACK

JIN-WEON KIM
Department of Nuclear Engineering, Chosun University
375 Seosuk-dong, Dong-gu, Gwangju, Korea
E-mail : jwkim@chosun.ac.kr

Received August 21, 2006
Accepted for Publication November 7, 2006

This paper presents a closed-form model for evaluating the restraint effect of pressure induced bending on the opening of a circumferential through-wall crack, which is considered plastic deformation behavior. Three-dimensional finite element analyses with different crack lengths, restraint conditions, pipe geometries, magnitudes of internal pressure, and tensile properties were used to investigate the influence of each parameter on the pressure-induced bending restraint on the crack opening displacement. From these investigations, an analytical model based on elastic-perfectly plastic material was developed in terms of the crack length, symmetric restraint length, mean radius to thickness ratio, axial stress corresponding to the internal pressure, and normalized crack opening displacement evaluated from a linear-elastic crack opening condition. Finite element analyses results demonstrate that the proposed analytical model reliably estimated the restraint effect of pressure-induced bending on the plastic crack opening of a circumferential through-wall crack and properly reflected the dependence on each parameter within the range over which the analytical expression was derived.

KEYWORDS : Closed-Form Model, Plastic Crack Opening, Pressure Induced Bending, Restraint Effect, Finite Element Analysis, Leak-Before-Break Analysis

1. INTRODUCTION

Current pipe crack evaluation procedures, including leak-before-break (LBB) analyses, assume that a cracked pipe, which is subjected to remote bending and internal pressure, is free to rotate [1,2]. In this case, the axial load from the internal pressure induces bending of the pipe due to the eccentricity of the neutral axis in the cracked plane versus the center of an uncracked pipe. This pressure-induced bending (PIB) promotes opening of a circumferential through-wall crack (TWC) in the pipe. In a real piping system, however, the PIB is restrained because the ends of the pipe are constrained by the rest of the piping system and other components. Hence, the existing evaluation procedures, which do not consider the restraint of PIB, overestimate the crack opening displacement (COD) of a circumferential TWC in a real piping system [3,4]. This overestimation comprises one of the uncertainties in an LBB analysis, as it leads to underprediction of the leakage-size-crack (LSC) length of a postulated TWC, and thus results in a non-conservative estimation of the crack stability [4,5].

Therefore, it is necessary to quantitatively evaluate the restraint effect of PIB on the COD of a circumferential TWC in order to ensure the reliability of the current LBB analysis procedures and the applicability of the LBB concept to nuclear piping systems. Recently, several studies evaluated the restraint effect of PIB on COD, and proposed a simplified model to evaluate the COD under restrained conditions [6,7]. However, these results are quite limited in terms of their applicability, because the restraint effect was evaluated only in terms of a linear-elastic crack opening. In practice, a circumferential TWC in a pipe behaves plastically under normal operating loads, and current LBB analysis methodologies require an elastic-plastic crack opening evaluation [1,8]. In addition, our previous study showed that the restraint effect of PIB on the COD is more significant when plastic behavior is considered than when a linear-elastic crack opening behavior is assumed [9,10]. When considering plastic deformation, the restraint

effect is influenced by the magnitude of the internal pressure, in contrast with linear-elastic analysis results.

The objective of this study is to develop a closed-form model to evaluate the restraint effect of PIB on the plastic crack opening of a circumferential TWC in a pipe. Using elastic-plastic finite element analyses, this study evaluates the restraint effect of PIB on the COD under various conditions including the crack length, restraint length, pipe geometry, and material properties. From the results of the analyses, the dependence of the restraint effect of PIB on each influencing parameter is investigated and key parameters are determined to develop the model. Based on these investigations and additional elastic-perfectly plastic finite element analyses, an analytical model to quantitatively estimate the restraint effect of PIB on plastic crack opening is proposed and its validity is evaluated.

2. EVALUATION PROCEDURE

2.1 Evaluation Method

In order to evaluate the restraint effect of PIB on the COD, a TWC was considered in a pipe with mean radius (R_m), wall thickness (t), and initial crack angle (2θ) as illustrated in Fig. 1. The pipe was subjected to an axial tension load (T) corresponding to an internal pressure (P) with and without the restraint of pressure induced bending at a distance (L_R and L_R') on either side of the cracked plane. L_R and L_R' are restraint lengths defined simply by the locations of the restrained pipe cross-sections from the cracked plane.

The restraint effect of PIB on the COD, which can be considered plastic behavior, was quantified by normalizing a restrained COD (δ_R) with an unrestrained COD (δ_F), as represented by

$$r_{COD,P} = \delta_R / \delta_F \quad (1)$$

Thus, the restraint effect of PIB on the COD is significant when $r_{COD,P}$ approaches zero, and the effect is negligible when $r_{COD,P}$ approaches one. In the present study, both restrained and unrestrained CODs were computed by finite element analyses. The value of δ_F was calculated by applying the axial tensile stress equivalent to the internal pressure at cross-sections A-A and A'-A' under the conditions of free rotation, which is a typical analysis procedure. The value of δ_R was also calculated by applying the axial tensile stress to cross-sections A-A and A'-A' under the restraining condition simulated by the boundary conditions in the models.

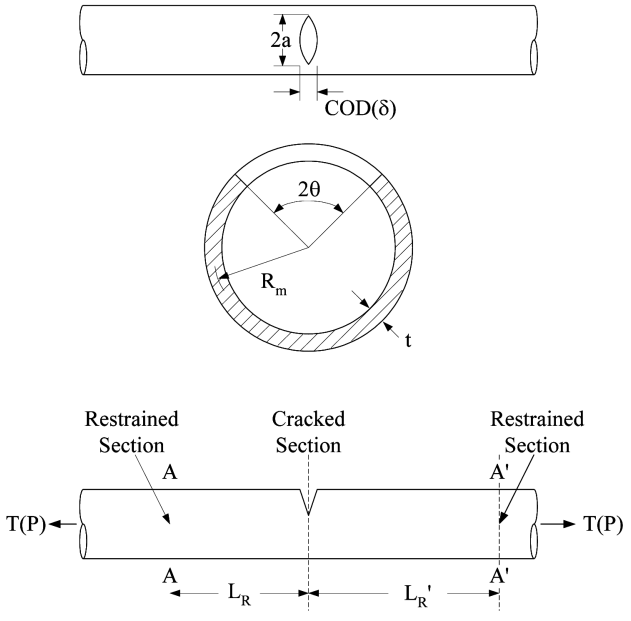

Fig. 1. Schematic Diagrams of a Circumferential Through-wall Cracked Pipe under PIB Restraint Conditions

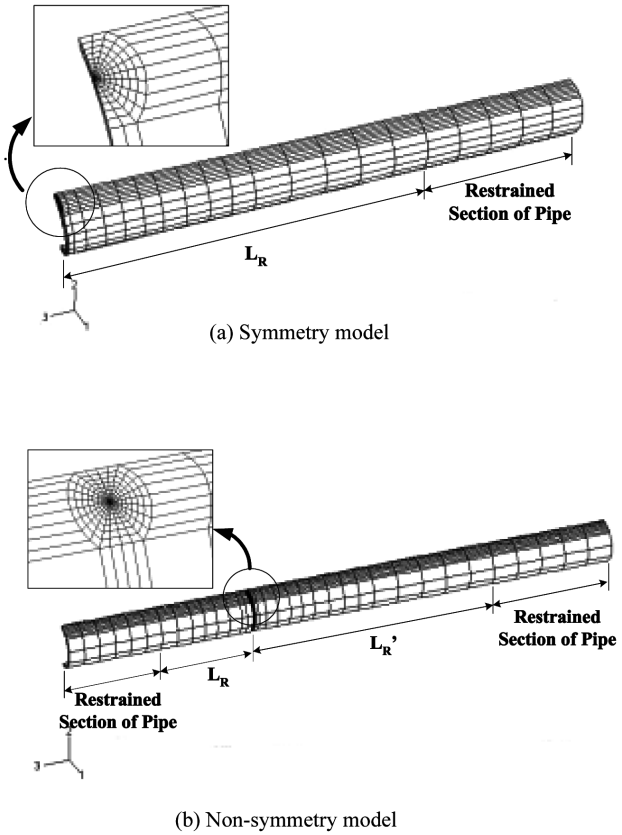

Fig. 2. Finite Element Models for COD Calculations

Table 1. Analysis Matrix Considered in the Present Study

D_m (mm)	R_m/t	Crack Length (θ/π)			Restraint Length (L_R'/D_m)				Restraint Length (L_R/D_m)
					1	5	10	20	
323.9	5	1/8	1/4	1/2	√	√	√	√	1
323.9	5	1/8	1/4	1/2		√	√	√	5
323.9	5	1/8	1/4	1/2			√	√	10
323.9	5	1/8	1/4	1/2				√	20
323.9	10	1/8	1/4	1/2	√	√	√	√	1
323.9	10	1/8	1/4	1/2		√	√	√	5
323.9	10	1/8	1/4	1/2			√	√	10
323.9	10	1/8	1/4	1/2				√	20
323.9	20	1/8	1/4	1/2	√	√	√	√	1
323.9	20	1/8	1/4	1/2		√	√	√	5
323.9	20	1/8	1/4	1/2			√	√	10
323.9	20	1/8	1/4	1/2				√	20

2.2 Finite Element Models

Elastic-plastic analyses were performed to evaluate the COD in a circumferential through-wall cracked pipe using ABAQUS, a general purpose finite element program [11]. Two types of finite element models were employed, as shown in Fig. 2. One made use of a quarter model to simulate the symmetrically restrained cracked pipe ($L_R = L_R'$), while the other made use of a half model to simulate the non-symmetrically restrained cracked pipe ($L_R \neq L_R'$). Two elements were used through the thickness for both models, and the CODs were determined from the displacement of the mid-thickness node at the center of the crack mouth. To avoid problems associated with incompressibility, reduced integration 20-node elements were used. The geometric nonlinearity effects due to large rotation and large strain were ignored.

In the analysis, only an axial tensile stress equivalent to the internal pressure was considered as the applied load. The effects of the pressure applied to the crack faces, hoop stress, and bending stress on the crack opening were ignored in the analysis. For the symmetric model, an equivalent tensile stress was applied to the elements located at L_R under symmetric boundary conditions. For the non-symmetric model, the tensile stress was applied to the elements located at distances L_R and L_R' from the cracked plane. The restraint on the pipe rotation in the models was considered by constraining the displacements, except in the longitudinal direction, of all nodes within a certain length of pipe beyond L_R and L_R', as illustrated in Fig. 2.

3. RESULTS OF THE PIB RESTRAINT EFFECT ANALYSIS

Previous studies, based on linear-elastic analyses, showed that the restraint effect of PIB on the COD is a function of the normalized crack length (θ/π), mean radius to thickness ratio (R_m/t), and restraint lengths normalized by the mean diameter of the pipe (L_R/D_m, L_R'/D_m) [6]. Thus, the present study evaluated the normalized COD, $r_{COD,P}$, under various conditions using elastic-plastic finite element analyses to clarify the dependence of the PIB restraint effect on these influencing parameters and to determine the key parameters to be included in the analytical model. Table 1 summarizes the analysis conditions of each parameter considered in this study. Several types of true stress-strain curves, shown in Fig. 3 and obtained from base and weld metals of austenitic stainless steel, cast stainless steel, and ferritic steel, were also considered in the analysis. The reference true stress-strain curve given in Fig. 3 was used to evaluate the dependence on crack length, restraint length, and radius to thickness ratio. All true stress-strain curves were considered to evaluate the effect of material properties on the restraint effect of PIB. A bi-linear fully plastic curve with a Young's modulus of 200GPa and yield stress of 200MPa, also presented in Fig. 3, was used in the elastic-perfectly plastic analysis.

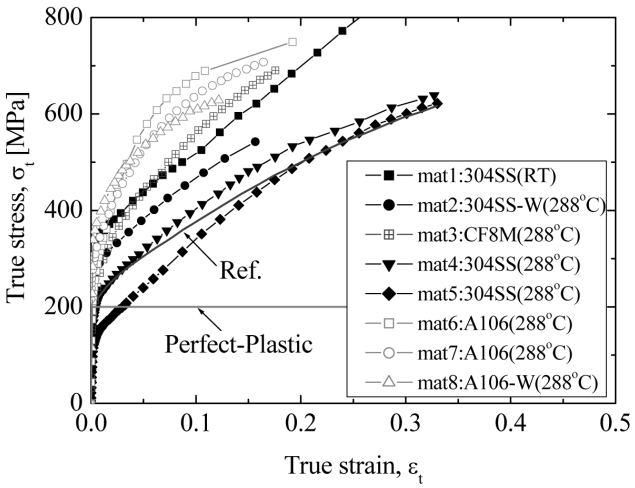

Fig. 3. True Stress versus Strain Curves Used in the Finite Element Analysis

3.1 Evaluation of the PIB Restraint Effect for Each Parameter

Figure 4 presents the $r_{COD,P}$ evaluated from different crack lengths, θ/π = 1/8, 1/4, 1/2 and symmetric restraint lengths, L_R/D_m = 1 and 10, as a function of the applied axial stress (σ_{app}) corresponding to internal pressure. The results show that $r_{COD,P}$ decreased, regardless of stress level, with increasing crack length and with decreasing symmetric restraint length. That is, the restraint effect of PIB on the plastic COD was considerable for a larger crack length and shorter restraint length. This tendency is consistent with that observed in linear-elastic analysis results [3,4,6]. However, in contrast with the linear-elastic analysis results, the restraint effect of PIB in this case was strongly dependent on the magnitude of the internal pressure. As the axial stress equivalent to internal pressure increased, $r_{COD,P}$ dramatically decreased above a critical internal pressure. The critical internal pressure required to initiate this phenomenon decreased with increasing crack length, but was independent of the restraint length. When the applied axial stress equivalent to the internal pressure approached zero, the value of $r_{COD,P}$ reached $r_{COD,E}$, the normalized COD calculated from the linear-elastic analysis.

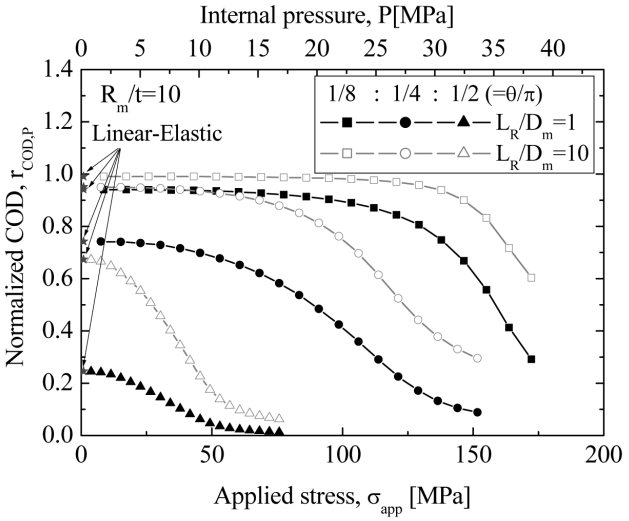

Fig. 4. Dependence of the Normalized COD, $r_{COD,P}$, on the Crack Length, Symmetric Restraint Length, and Applied Axial Stress Equivalent to Internal Pressure

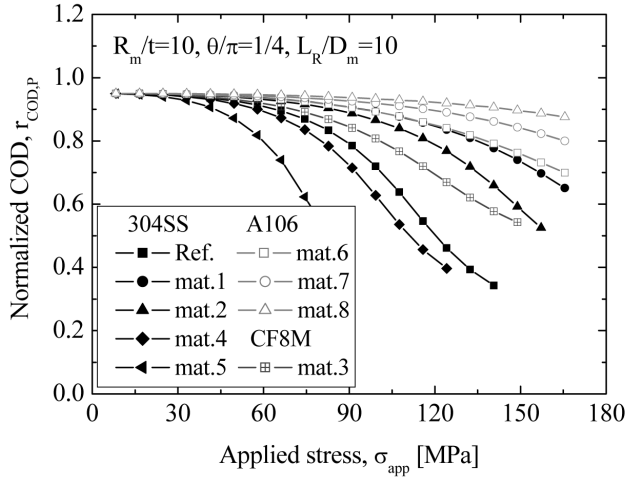

Fig. 5. Dependence of the Normalized COD, $r_{COD,P}$, on the True Stress versus Strain Curves of the Material

To investigate the influence of the material properties on the restraint effect of PIB on the plastic COD, the value of $r_{COD,P}$ was calculated using the true stress-strain curves exhibited in Fig. 3 for a given pipe geometry (R_m/t=10), crack length (θ/π = 0.25), and symmetric restraint length (L_R/D_m =10), and the results were compared. As shown in Fig. 5, the value of $r_{COD,P}$ was strongly dependent on the true stress-strain curve used in the analysis. In particular, the dependence of $r_{COD,P}$ on the true stress-strain curve became significant for higher applied axial stresses. Comparing this result with the tensile properties, such as the yield stress, flow stress, and tensile stress of each material, the value of $r_{COD,P}$ at a given stress level was found to be proportional to the yield stress of the pipe material. This implies that the restraint effect of PIB on plastic crack opening of a circumferential TWC is less significant for a pipe with a higher yield stress.

According to the results of a previous study that considered plastic crack behavior [10], the dependence of $r_{COD,P}$ on the magnitude of the internal pressure and on the tensile properties is associated with the characteristic that the restraint effect of PIB on the COD is governed by the stress state in the crack ligament. With increasing applied axial stress, the stress state in the crack ligament changes from an elastic to plastic regime for an unrestrained cracked pipe, unlike a restrained cracked pipe. Thus, the stiffness of the pipe at the cracked section for unrestrained conditions decreases considerably above a critical axial stress, which depends on the circumferential crack length, and $r_{COD,P}$ is abruptly reduced. This is also evidenced by the fact that the value of $r_{COD,P}$ at a given applied stress is proportional to the yield stress of the pipe material.

3.2 Simplifying the Dependence on Influencing Parameters

As described in the previous section, the restraint effect of PIB on the plastic crack opening of a circumferential TWC is governed by the stress state in the crack ligament. Also, the value of $r_{COD,P}$ reaches $r_{COD,E}$ when the internal pressure is reduced to zero. Therefore, the analysis results can be simplified by normalizing $r_{COD,P}$ and the applied axial stress with $r_{COD,E}$ and a collapse stress at a cracked section defined by

$$\sigma_C = \frac{\sigma_y}{\pi}\left[\pi - \theta - 2\sin^{-1}(0.5\sin\theta)\right] \quad (2)$$

where σ_y is the yield stress of material and θ is the half angle of the circumferential TWC depicted in Fig. 1. Thus, the restraint effect of PIB on plastic crack opening, $r_{COD,P}$, is represented by a relative value of the restraint effect of PIB evaluated from linear-elastic crack opening conditions ($r_{COD,E}$).

Figures 6 ~ 8 present the normalizing factor, $r_{COD,P}/r_{COD,E}$, as a function of the normalized applied stress (σ_{app}/σ_C) for different crack lengths and symmetric restraint lengths, pipe geometries, and non-symmetric restraint lengths. By comparing Fig. 6 with Fig. 4, the dispersion of $r_{COD,P}$ with crack length and symmetric restraint length was apparently reduced by the normalization. In Figs. 6 and 7, the overall patterns of the $r_{COD,P}/r_{COD,E}$ versus σ_{app}/σ_C curves are dominated by the crack length, and the symmetric restraint length and pipe geometry only affect the value of $r_{COD,P}/r_{COD,E}$ at a given normalized applied stress level. The effect of the non-symmetric restraint length of $r_{COD,P}/r_{COD,E}$ is negligible, as shown in Fig. 8. Therefore, the normalized applied stress, crack length, symmetric restraint length, and R_m/t of the pipe should be the main parameters in the development of an analytical model. The non-symmetric restraint length can be ignored.

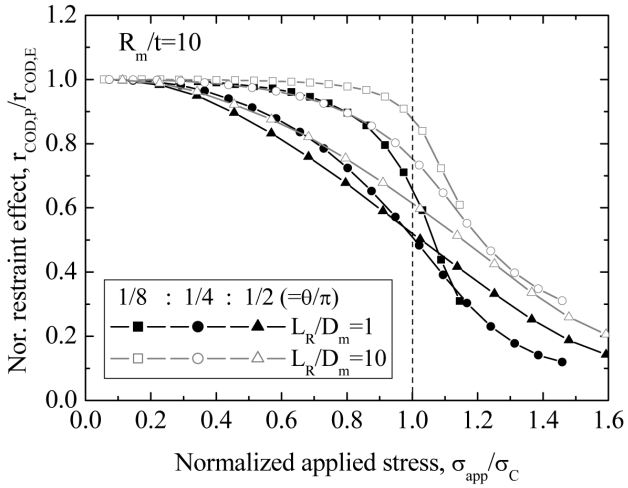

Fig. 6. Effect of the Crack Length and Symmetric Restraint Length on the $r_{COD,P}/r_{COD,E}$ versus σ_{app}/σ_C Curves

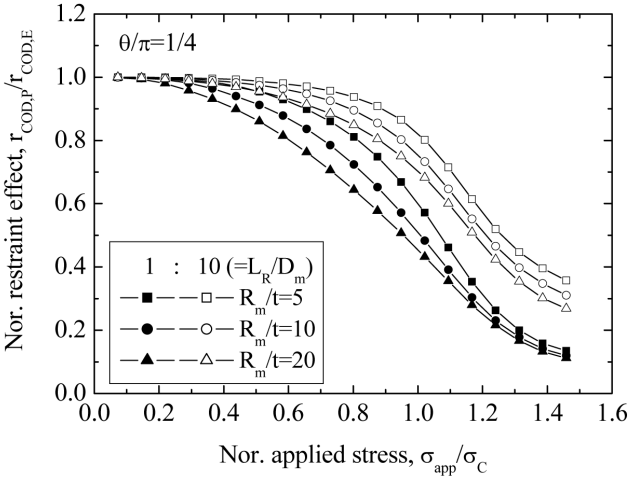

Fig. 7. Effect of the Mean Radius to Thickness Ratio on the $r_{COD,P}/r_{COD,E}$ versus σ_{app}/σ_C Curves

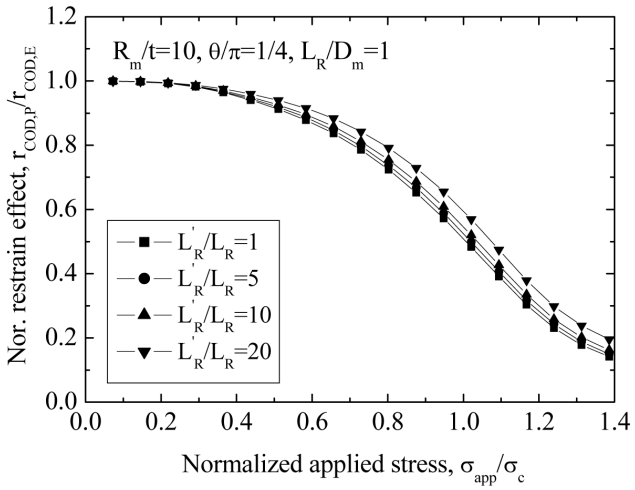

Fig. 8. Effect of the Non-symmetric Restraint Length on the $r_{COD,P}/r_{COD,E}$ versus σ_{app}/σ_C Curves

The normalization also reduced the dependence of $r_{COD,P}$ on the true stress-strain curve used in the analysis. As shown in Fig. 9, the $r_{COD,P}/r_{COD,E}$ versus σ_{app}/σ_C curve was nearly identical for the same grade material, although the difference between true stress-strain curves was considerable. When the type of material was changed, however, the discrepancy of $r_{COD,P}/r_{COD,E}$ still appeared in the higher stress region. This is associated with different strain hardening characteristics of the material. In this study, therefore, the behavior of the material is assumed to be fully plastic in order to exclude different strain hardening characteristics. Figure 10 presents a comparison of the normalizing factor, $r_{COD,P}/r_{COD,E}$, evaluated for elastic-plastic and elastic-perfectly plastic material conditions. The $r_{COD,P}/r_{COD,E}$ values obtained for both conditions were nearly the same at lower applied stresses ($\sigma_{app}/\sigma_C < 0.5$), regardless of the strain hardening characteristic; the differences between $r_{COD,P}/r_{COD,E}$ appeared at $\sigma_{app}/\sigma_C > 0.5$. In the elastic-perfectly plastic analysis,

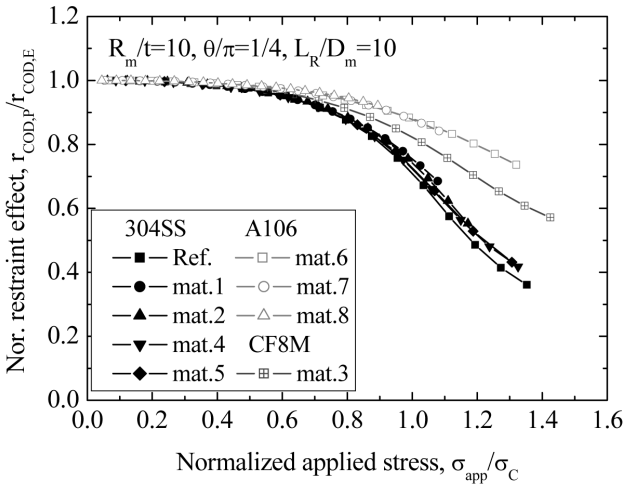

Fig. 9. Effect of the Stress versus Strain Curves on the Normalized Restraint Effect, $r_{COD,P}/r_{COD,E}$

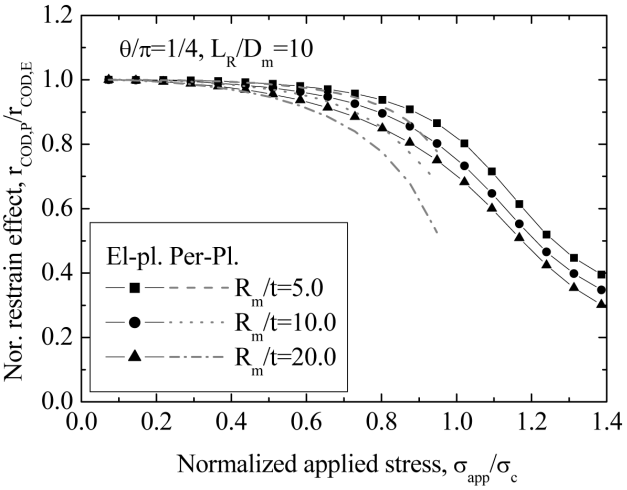

Fig. 10. Comparison of $r_{COD,P}/r_{COD,E}$ Obtained from Elastic-Plastic and Elastic-perfectly Plastic Finite Element Analyses

$r_{COD,P}/r_{COD,E}$ is meaningless for $\sigma_{app}/\sigma_C > 1.0$, because the cracked section of pipe collapses when the applied stress exceeds the collapse stress.

Although a discrepancy between $r_{COD,P}/r_{COD,E}$ was obvious in the higher stress region, the dependence of $r_{COD,P}/r_{COD,E}$ on the crack length, symmetric restraint length, and R_m/t in the elastic-perfectly plastic analysis was consistent with those observed from the elastic-plastic analysis that considered the actual strain hardening characteristics of the material. In addition, the value of $r_{COD,P}/r_{COD,E}$ from the elastic-perfectly plastic analysis was always less than that from the elastic-plastic analysis. Thus, the perfectly plastic assumption provided a reasonable estimate of the dependence on each parameter and gave conservative results.

4. DEVELOPMENT OF AN ANALYTICAL MODEL

4.1 Derivation of an Analytical Model

In the previous section, it was recognized that the overall pattern of the $r_{COD,P}/r_{COD,E}$ versus σ_{app}/σ_C curves was mainly governed by the crack length, and the value of $r_{COD,P}/r_{COD,E}$ for a given σ_{app}/σ_C was dependent on the symmetric restraint length and pipe geometry. Also, the dependence of the restraint effect of PIB on the material properties could be eliminated by assuming that the plastic behavior of the material was fully plastic. Therefore, the normalizing factor, $r_{COD,P}/r_{COD,E}$, can be simply expressed as a function of σ_{app}/σ_C, θ/π, L_R/D_m, R_m/t :

$$\frac{r_{COD,P}}{r_{COD,E}} = f\left(\frac{\sigma_{app}}{\sigma_C}, \frac{\theta}{\pi}, \frac{L_R}{D_m}, \frac{R_m}{t}\right) \tag{3}$$

The relationship between $r_{COD,P}/r_{COD,E}$ and its influencing parameters, σ_{app}/σ_C, θ/π, L_R/D_m and R_m/t, can be derived from the results of elastic-perfectly plastic finite element analyses performed under various conditions. The analysis matrix considered was the same as that given in Table 1, except that $L_R/D_m = 40$ was added to the symmetric restraint length and the non-symmetric restraint condition was excluded. From these analyses results, the following analytical model was derived:

$$\frac{r_{COD,P}}{r_{COD,E}} = 2.0 - \exp\left[A\left(\frac{\sigma_{app}}{\sigma_C}\right)^B\right] \quad for\ \frac{\sigma_{app}}{\sigma_C} \le 1.0$$

$$\frac{r_{COD,P}}{r_{COD,E}} = 0.0 \quad for\ \frac{\sigma_{app}}{\sigma_C} > 1.0 \tag{4}$$

Since the restraint effect is meaningless when the applied stress exceeds the collapse stress, the $r_{COD,P}/r_{COD,E}$ was expressed as zero for $\sigma_{app}/\sigma_C > 1.0$. In the range of $0.0 \le \sigma_{app}/\sigma_C \le 1.0$, an analytical expression was derived by regression of the analysis results. Thus, the analytical expression represented by Eq. (4) shows discontinuity at $\sigma_{app}/\sigma_C = 1.0$.

The coefficients A and B in Eq. (4) are functions of the crack length, symmetric restraint length, and R_m/t of the pipe as follows:

$$A = \alpha_0 + \alpha_1\left(\frac{\theta}{\pi}\right) + \alpha_2\left(\frac{\theta}{\pi}\right)^2$$

$$\alpha_i = \alpha_{i0} + \alpha_{i1}\ln\left(\frac{L_R}{D_m}\right) + \alpha_{i2}\ln^2\left(\frac{L_R}{D_m}\right),\ i = 0, 1, 2$$

$$\alpha_{ij} = a_{ij} + b_{ij}\left(\frac{R_m}{t}\right) + c_{ij}\left(\frac{R_m}{t}\right)^2,\ i, j = 0, 1, 2 \quad (5)$$

$$B = 1/\left[\beta_0 + \beta_1\left(\frac{\theta}{\pi}\right) + \beta_2\left(\frac{\theta}{\pi}\right)^2\right]$$

$$\beta_i = \beta_{i0} + \beta_{i1}\exp\left[\beta_{i2}\left(\frac{L_R}{D_m}\right)\right],\ i = 0, 1, 2$$

$$\beta_{ij} = u_{ij} + v_{ij}\left(\frac{R_m}{t}\right) + w_{ij}\left(\frac{R_m}{t}\right)^2,\ i, j = 0, 1, 2 \quad (6)$$

The constants, a_{ij}, b_{ij}, c_{ij}, u_{ij}, v_{ij} and w_{ij}, are listed in Table 2. Therefore, the restraint effect of PIB on the plastic COD, $r_{COD,P}$, for a given internal pressure, pipe geometry, circumferential crack length, and symmetric restraint length, can be estimated from Eq. (4) by inserting the value of $r_{COD,E}$ provided by the existing model based on a linear-elastic analysis [6].

Table 2. Constants in Eqs. (5) and (6)

Constants	Values
a_{00}, b_{00}, c_{00}	-0.21508, 0.06082, -0.00147
a_{01}, b_{01}, c_{01}	-0.03544, -0.01256, 5.77533×10^{-4}
a_{02}, b_{02}, c_{02}	0.02114, -0.00120, -3.18667×10^{-5}
a_{10}, b_{10}, c_{10}	3.02600, -0.16596, 0.00337
a_{11}, b_{11}, c_{11}	-0.43042, 0.11201, -0.00418
a_{12}, b_{12}, c_{12}	-0.10104, -0.00463, 5.14067×10^{-4}
a_{20}, b_{20}, c_{20}	-3.90640, 0.18586, -0.00356
a_{21}, b_{21}, c_{21}	1.05512, -0.17493, 0.00615
a_{22}, b_{22}, c_{22}	0.03891, 0.01553, -9.32933×10^{-4}
u_{00}, v_{00}, w_{00}	0.01754, -0.00138, 1.23000×10^{-4}
u_{01}, v_{01}, w_{01}	0.00613, -0.01483, 2.21200×10^{-4}
u_{02}, v_{02}, w_{02}	0.00364, -0.01261, 4.84133×10^{-4}
u_{10}, v_{10}, w_{10}	0.67554, -0.01968, 4.05200×10^{-4}
u_{11}, v_{11}, w_{11}	0.08664, 0.29072, -0.00608
u_{12}, v_{12}, w_{12}	-0.13326, -0.00234, 1.81800×10^{-4}
u_{20}, v_{20}, w_{20}	-0.43146, 0.11374, -0.00274
u_{21}, v_{21}, w_{21}	0.00810, -0.48323, 0.01035
u_{22}, v_{22}, w_{22}	-0.27404, 0.00883, -1.10867×10^{-4}

4.2 Verification of the Proposed Model

4.2.1 Reliability of the Proposed Model

To evaluate the reliability of the model proposed in this work, the results predicted by Eq. (4) were compared with elastic-perfectly plastic finite element analysis results. Figure 11 compares different circumferential crack lengths, symmetric restraint lengths, and R_m/t of the pipe. The value of $r_{COD,P}/r_{COD,E}$ predicted by the analytical model agrees well with the finite element analysis results over all the ranges of applied stress (σ_{app}/σ_C = 0.0~1.0), regardless of the crack length, restraint length, and R_m/t of pipe. The same level of accuracy was observed for $0.125 \le \theta/\pi \le 0.5$, $1.0 \le L_R/D_m \le 40.0$ and $5 \le R_m/t \le 20$, the range over which the analytical model was derived. Thus, the proposed model reliably estimated the restraint effect of PIB on the plastic crack opening of a circumferential TWC within the range over which the analytical expression was derived.

The analytical model was based on an assumption of elastic-perfectly plastic material. In practice, however, pipe material shows non-linear elastic-plastic behavior with a strain hardening characteristic. Thus, the reliability and conservatism of the proposed model were verified by comparing the results obtained from the proposed model and those from an elastic-plastic finite element analysis. Figure 12 shows the comparisons, which are quantitatively represented as deviation of the value of $r_{COD,P}/r_{COD,E}$ from the results of a elastic-plastic finite element analysis that considered strain hardening characteristics of the material, together with the results obtained from the existing model proposed on the basis of a linear-elastic material condition. In Fig. 12, a negative deviation means that the model overestimates the restraint effect of PIB on COD whereas a positive deviation means that the model underestimates the restraint effect of PIB on COD, i.e., non-conservative estimation. As shown in Fig. 12, with increasing applied axial stress, the deviation of $r_{COD,P}/r_{COD,E}$ increased for both analytical models. However, the degree of deviation in the present model was much smaller, about 2 ~ 3 times,

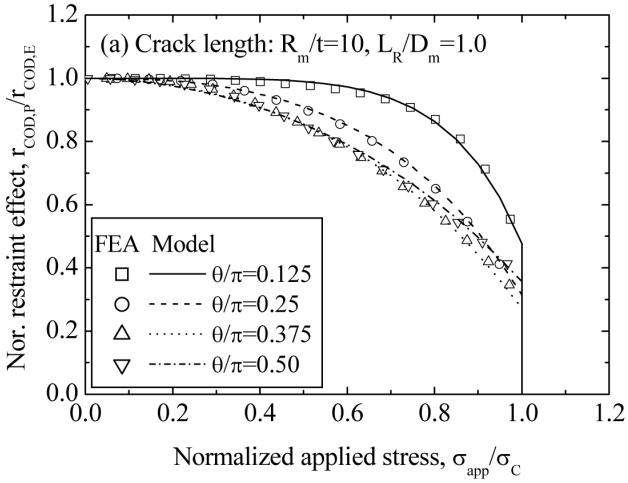

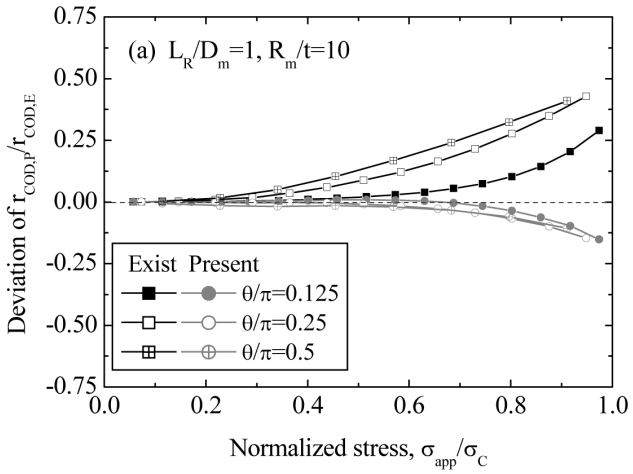

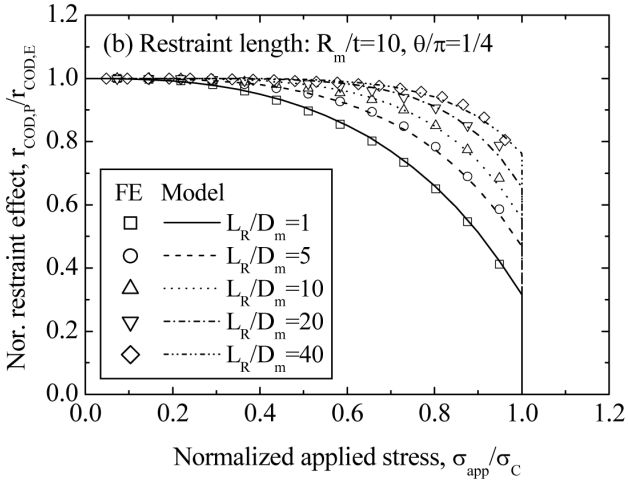

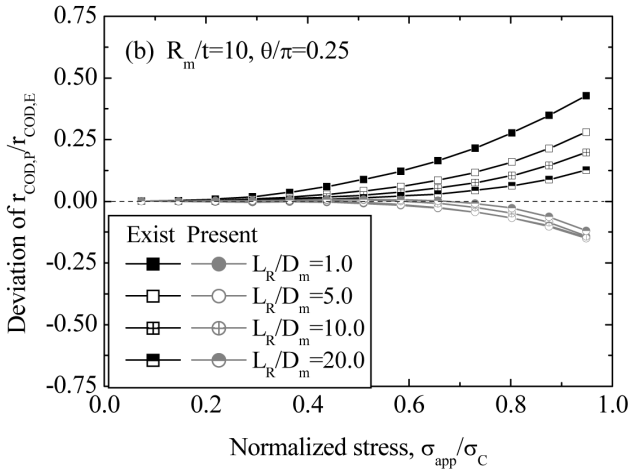

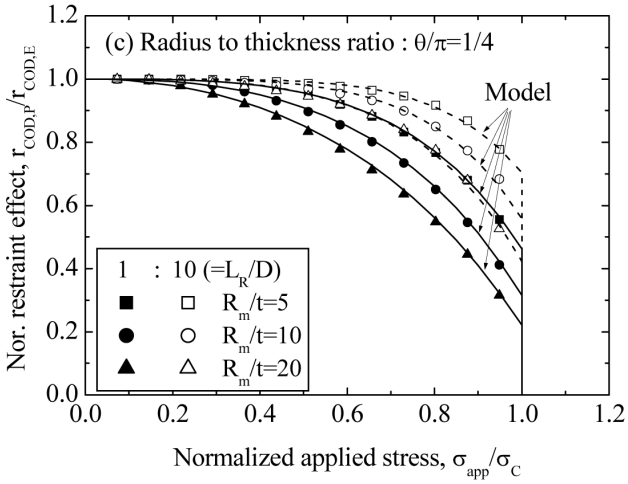

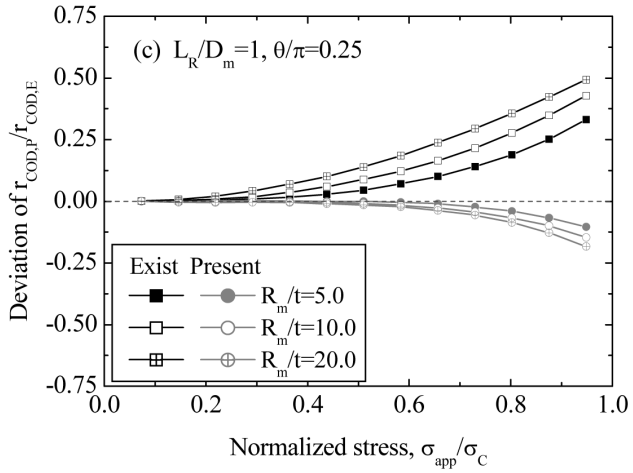

Fig. 11. Comparison of $r_{COD,P}/r_{COD,E}$ Obtained from the Proposed Analytical Model and Elastic-perfectly Plastic Finite Element Analysis

Fig. 12. Deviation of $r_{COD,P}/r_{COD,E}$ Predicted by the Existing and Present Analytical Models from the Elastic-plastic Finite Element Analysis Results

than that in the existing linear-elastic analysis based model. Also, the present model always gave a negative value of deviation, reflecting conservative estimation of the restraint effect of PIB on COD, in contrast with the existing linear-elastic based model, which showed positive deviation. Therefore, it is found that, in comparison with the existing model, the present model accurately and conservatively estimates the restraint effect of PIB on the COD, even though it was developed on the basis of an elastic-perfectly plastic material assumption.

4.2.2 Dependence on Each Influencing Parameter

In order to confirm whether the proposed analytical model reflects the dependence on each influencing parameter and has continuity over the range of interest, the values of $r_{COD,P}/r_{COD,E}$ were evaluated for a given applied axial stress, and the resulting variation with each influencing parameter was examined. Figure 13 displays the variation of $r_{COD,P}/r_{COD,E}$ with the crack length, restraint length, and R_m/t of pipe at $\sigma_{app}/\sigma_C = 0.5$. No discontinuities in the analytical expressions were observed in the figure over the full range of each parameter. In Fig. 13(a), the value of $r_{COD,P}/r_{COD,E}$ was nearly one for a small crack length, regardless of the symmetric restraint length, but this value decreased with increasing crack length. The decrease in $r_{COD,P}/r_{COD,E}$ was significant for a shorter restraint length. For a given crack length ($\theta/\pi = 0.25$), as shown in Fig. 13(b), the value of $r_{COD,P}/r_{COD,E}$ sharply increased initially and then converged to one with increasing symmetric restraint length. As R_m/t decreased, the value of $r_{COD,P}/r_{COD,E}$ converged at a shorter restraint length. Also, the value of $r_{COD,P}/r_{COD,E}$ almost linearly decreased with increasing R_m/t of the pipe (see Fig. 13(c)). For a small size crack ($\theta/\pi = 0.125$), the dependence of $r_{COD,P}/r_{COD,E}$ on R_m/t was negligible, but it became apparent with increasing circumferential crack length. The dependence on each influencing parameter was consistent with that observed in the finite element analysis results [9,10]. Thus, the proposed analytical model appropriately reflects the dependence of the restraint effect of PIB on the plastic crack opening on each influencing parameter.

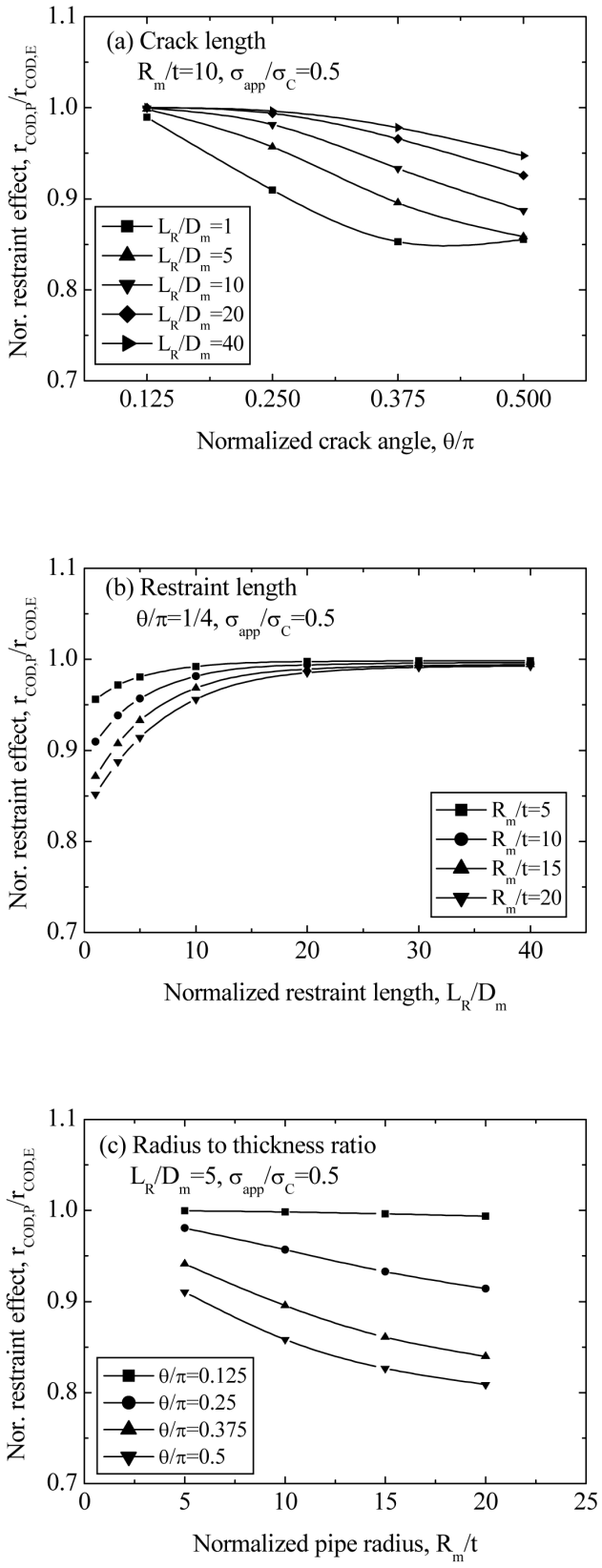

Fig. 13. Dependence of $r_{COD,P}/r_{COD,E}$ Predicted by the Proposed Model on the Influencing Parameters

5. CONCLUSIONS

The present study proposed an analytical model to evaluate the restraint effect of PIB on the plastic crack opening of a circumferential through-wall crack in a pipe. In order to develop the model, elastic-plastic and elastic-perfectly plastic finite element analyses were performed under various conditions. The results of these parametric analyses were used to investigate the dependence of the pressure-induced bending restraint effect on each influencing parameter, and an analytical model based on an elastic-perfectly plastic material was derived. The proposed analytical model reliably estimated the restraint effect of PIB on plastic crack opening of a circumferential through-wall

crack in a restrained pipe within the range investigated: $0.125 \leq \theta/\pi \leq 0.5$, $1.0 \leq L_R/D_m \leq 40.0$ and $5 \leq R_m/t \leq 20$. The model also appropriately reflected the dependence on the influencing parameters. Therefore, the proposed analytical model can be applied to evaluate the leakage-size-crack length in a leak-before-break analysis that considers plastic crack opening behavior. Furthermore, the uncertainty introduced by the restraint effect of PIB on crack opening in the current LBB analysis procedure can be improved.

REFERENCES

[1] Pipe Break Task Group, 1984, "Evaluation of Potential for Pipe Breaks," *NUREG-1061*, Vol. 3.

[2] Zahoor, A., 1989, "Ductile Fracture Handbook," EPRI NP-6301-D.

[3] Rahman, S., Ghadiali, N., Wilkowski, G., Moberg, F. and Brickstad, B., 1998, "Crack-Opening-Area Analyses for Circumferential Through-Wall Cracks in Pipes - Part III: Off-Center Cracks, Restraint of Bending, Thickness Transition and Weld Residual Stresses," *Int. J. Press. Ves. & Piping*, Vol. 75, pp. 397-415.

[4] Ghadiali, S., Rahman, S., Choi, Y.H. and Wilkowski, G.M, 1996, "Deterministic and Probabilistic Evaluations for Uncertainty in Pipe Fracture Parameters in Leak-Before-Break and In-Service Flaw Evaluations," *NUREG/ CR-6443*.

[5] Wilkowski, G., Olson, R. and Scott, P., 1997, "State-of the-Art Report on Piping Fracture Mechanics," *NUREG/CR-6540*.

[6] Scott, P., Olson, R., Bockbrader, J., Wilson, M., Gruen, B., Morbitzer, R., Yang, Y., Williams, C., Burst, F., Fredette, L. and Ghadiali, N., 2005, "The Battelle Integrity of Nuclear Piping (BINP) Program Final Report," *NUREG/CR-6837*.

[7] Miura, N., 2001, "Evaluation of Crack Opening Behavior for Cracked Pipes Effect of Restraint on Crack Opening," *ASME-PVP*, Vol.423, pp. 135-143.

[8] Norris, D.M. and Chexal, B., 1987, PICEP : Pipe Crack Evaluation Program (Revision 1), EPRI NP-3596-SR, Rev.1.

[9] Kim, J.W. and Park, C.Y., 2001, "Effect of Restraint of Pressure Induced Bending on Crack Opening Evaluation for Circumferential Through-Wall Cracked Pipe," *Trans. of KSME (A)*, Vol.25, No.11, pp.1873-1880.

[10] Kim, J.W., 2004, "Evaluation of Restraint Effect of Pressure Induced Bending on the Elastic-Plastic Crack Opening Behavior," *Int. J. Press. Ves. & Piping*, Vol. 81, pp. 355-362.

[11] ABAQUS Users manual, version 6.3, Hibbitt, Karlson & Sorensen, 2000.